12th International Conference on Fracture Mechanics of Concrete and Concrete Structures
FraMCoS-12
B.L.A. Pichler, Ch. Hellmich, P. Preinstorfer (Eds)

https://doi.org/10.21012/FC12.1286
MS07-1:1

SELF-HEALING IN REACTIVE MAGNESIA CEMENT-BASED COMPOSITES UNDER DIFFERENT WATER-TO-BINDER RATIOS

DHANENDRA KUMAR[*], GU LEI[†] AND EN-HUA YANG[#]

[*] School of Civil and Environmental Engineering, Nanyang Technological University (NTU)
50 Nanyang Avenue, Singapore – 639798, Singapore
e-mail: dhanendra.kumar@ntu.edu.sg

[†] School of Civil and Environmental Engineering, Nanyang Technological University (NTU)
50 Nanyang Avenue, Singapore – 639798, Singapore
e-mail: gulei_edward@outlook.com

[#] School of Civil and Environmental Engineering, Nanyang Technological University (NTU)
50 Nanyang Avenue, Singapore – 639798, Singapore
e-mail: ehyang@ntu.edu.sg, https://dr.ntu.edu.sg//cris/rp/rp00775

Key words: Self-healing, Magnesium-based Cement, Carbonation Curing, Cracks, Durability.

Abstract: The water-to-binder (w/b) ratio is the prime factor governing the degree of hydration and composition of hydration products in cementitious composites. The hydrated phase composition consequently governs the performance of composites under different mechanical and environmental loadings. In this study, the effects of w/b ratios on the self-healing characteristics (under wetting-drying cycles) of carbonated reactive magnesia cement (RMC) based composites were investigated. This investigation focuses on the study of healed products and corresponding microstructure evolution. The study was conducted on RMC-based composites with w/b ratios of 0.30 and 0.40. The behavior was characterized on 7-day and 90-day matured composites to understand the effects on early-age crack mitigation and long-term performance simultaneously. The self-healing efficiency was characterized using crack width closure. The chemical characterization of the healing products was done using XRD and TGA analysis, and the morphology of the healing products was studied using SEM and EDS. The results demonstrate almost 100% crack closure in composites with a low w/b ratio than 80-90% crack closure at a high w/b ratio. The main healing product in low w/b RMC composite was amorphous magnesium-silicate-hydrate (MSH), whereas hydrated magnesium carbonates (HMCs) were observed in 0.40 w/b ratio RMC composite due to the increased porosity. The composition of healing products was different at the surface and core region of the healed matrix. The results will enable the tailoring of RMC-based composites to have desirable self-healing attributes.

1 INTRODUCTION

Reactive magnesia cement (RMC) has garnered significant attention recently due to its low calcination temperature (700°C) ability to sequester carbon [1, 2]. The RMC is a magnesium oxide (MgO) based binder that hardens and achieves mechanical strength when subjected to carbonation reaction, forming hydrated magnesium carbonates (HMCs) [3]. The commonly formed HMCs are hydromagnesite [$4MgCO_3 \cdot Mg(OH)_2 \cdot 4H_2O$], dypingite [$4MgCO_3 \cdot Mg(OH)_2 \cdot 5H_2O$], and nesquehonite [$MgCO_3 \cdot 3H_2O$]. The carbonation reactions explaining the formation of different HMCs are presented in the following references [1, 3-5]. The HMC

content depends on the mixture composition and curing conditions.

The RMC-based binder has been used by Ruan et al. [6] to develop Engineered Cementitious Composites (ECC) to combine the benefits of carbon sequestration and better tensile ductility, thus leading to the formation of cementitious composites with high durability and improved material sustainability. The ECC is a special class of fiber-reinforced concrete that exhibits tensile strain-hardening behavior through micromechanics-guided design principles [7, 8]. The tensile hardening is achieved through saturated multiple cracking in the composite with a typical crack width of less than 100 μm. This led to high tensile ductility in the material (more than 100 times that of conventional concrete) and provided high damage tolerance capabilities under various mechanical and environmental loadings [9].

The ECC has also shown notable autogenous self-healing capacity, which is attributed to its fine crack width [10-12]. Autogenous self-healing has been observed in conventional concrete but has rarely been significant due to the large crack width (typically > 200 μm). The fine crack width, an intrinsic material property of ECC, has led to its relevance in these composites [12]. The studies have reported significant recovery in the physical and mechanical properties of ECC through autogenous self-healing [13, 14]. The researchers have investigated the effects of environmental conditions and mixture composition on the self-healing efficiency of the ECC but limited to ordinary Portland cement (OPC) based composition.

The primary mechanism of autogenous healing in OPC-based ECC is the hydration of unreacted cement and the carbonation of calcium hydroxide in the hydrated phase (similar to that of OPC-based conventional concrete) [15-17]. The hydration and carbonation reactions led to additional portlandite, calcium-silicate-hydrate (C-S-H)), and calcite. The additional phases formed led to crack-sealing and the regain of composite stiffness. However, the change in the binder composition will alter the extent of self-healing due to the difference in the formation of new phases and their interactions/compatibility with the initial hydrated phase composition. The previous investigations have been mainly conducted on OPC-based compositions. The focus of this research is on RMC-based ECC.

The RMC-based ECC with a tensile strain capacity greater than 2% have been developed recently [6, 18]. The average crack has been reported as 67 μm and 58 μm, thus having significant potential for autogenous self-healing. Qiu et al. [19] have reported the self-healing potential of RMC-based ECC under various environmental exposure conditions. The study reported the necessity of water and higher CO_2 concentration for robust self-healing. The study showed that the healing products formed under different exposure conditions during self-healing regimes differed. It is thus expected that the change in initial binder composition would also affect the efficiency of self-healing in RMC-based ECC due to the change in hydrated phase composition and porosity (which affects the diffusion of CO_2 in the composite).

This research aimed to understand the effects of water-to-binder (w/b) weight ratio on the autogenous self-healing efficiency of RMC-based composite. The self-healing efficiency was characterized by surface crack-width recovery. The chemical and microstructural characterization of the healing products was conducted to understand the healing mechanisms. The experimental details and discussion of results are presented in the following sections.

2 MATERIALS AND METHODS

2.1 Materials

The composite utilized light-burnt reactive magnesia or magnesium-oxide (MgO) cement and Class F fly ash. The MgO weight content in RMC was 97%. The fly ash composition mainly includes SiO_2 (59.2%), Al_2O_3 (19.3%), Fe_2O_3 (7.1%), CaO (4.7%), and MgO (2.4%). The sodium hexametaphosphate (SHMP) or $[Na(PO_3)_6]$ dispersing agent was used as water

reducing agent. The 1.2% oil-coated polyvinyl alcohol (PVA) fiber, commonly used in ECC, was used at a 1% volume fraction [20]. The reduced volume fraction was used to suppress the multiple cracking tendency of the composite and allow a single crack. Two composites with w/b ratios of 0.30 and 0.40 were investigated in this study. The mixture composition is presented in Table 1. The properties of PVA fiber utilized are reported in Table 2.

Table 1: Mixture composition (by weight)

Mix ID	RMC	FA	Water (w/b)	SHMP
M-0.30	1.0	1.5	0.75 (0.30)	0.02
M-0.40	1.0	1.5	1.0 (0.40)	0.01

Table 2: Properties of PVA Fiber

Diameter (μm)	39
Length (mm)	12
Specific gravity	1.30
Tensile strength (MPa)	1600
Surface coating (oil content by wt. %)	1.2%

2.2 Sample preparation

The composites were prepared in a Hobart mixer. The RMC and fly ash were initially dry-mixed for three minutes. The SHMP was pre-dissolved in the mixing water content for 15 minutes. This water was added to the dry ingredients following dry mixing. The mixing was continued for another three minutes to achieve uniform consistency. The PVA fibers were then added slowly and mixed for five minutes. The mixture was poured in dogbone-shaped molds for crack-width characterization and additional chemical and microstructural characterization. The geometry of the dogbone specimen is shown in Figure 1.

The freshly prepared specimens (along with molds) were kept in a carbonation chamber at 30°C, 80% RH, and 10% CO_2. The specimens were demolded after 24 hours and cured under the same carbonation curing conditions in the carbonation chamber for 7 and 90 days. For individual mix, three specimens were prepared for each specimen age.

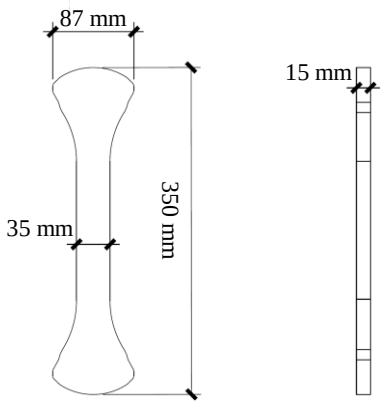

Figure 1: Dogbone specimen geometry.

2.3 Testing methodology

A single crack of width around 50±10 μm was induced in the dogbone specimens using displacement-controlled tensile loading at the rate of 0.1 mm/min. The exact crack width in each specimen after cracking was characterized using optical microscopy. The self-healing behavior was characterized using alternate wet-dry cycles. The wetting phase included submerging pre-cracked dogbone specimens in water (27±2°C) for 24 hours, and in drying phase, specimens were subjected to air drying in laboratory conditions (27±2°C, 80% RH) for 24 hours, following [19].

The crack width (at the surface of the specimen) was determined using optical microscopy (Optem microscope) after inducing a single crack and ten healing cycles. The crack-width recovery was quantified using the ratio of crack width reduction (i.e., difference in the original crack width and after ten healing cycles) divided by the original crack width (after inducing a single crack).

The morphology of the healed products in the cracked section and their EDS analysis were conducted using JEOL JSM-7600F field emission scanning electron microscope (SEM) in secondary electron (SE) imaging mode at 5 kV. The XRD (using Bruker D8 Advance diffractometer) and TGA (using PerkinElmer TGA 4000) analysis were conducted on powdered specimens. The powder sample for the bulk matrix was obtained from the uncracked matrix. The sample for characterizing healed products was obtained from one mm thin slice along the cracked

regions. The quantitative phase composition was determined using XRD with 5% calcium fluoride (CaF_2) as an external reference. The TGA was conducted in the 30-900°C temperature range at a 10°C/minute heating rate under an N_2 inert environment.

The additional detail of the experimental program is presented in [21].

3 RESULTS AND DISCUSSION

3.1 Crack width recovery

The efficiency of crack width recovery (after 10 wet-dry cycles) is summarized in Figure 2. The photos of crack closure after ten wet-dry cycles (observed using an optical microscope) are presented in Figure 3. The complete crack closure was observed in M-0.30 at all ages. The M-0.40 also demonstrated a high degree of crack closure (initial crack width of 50±10 µm) in the range of 3-5 µm in the 7-day and 8-12 µm in 90-day cured specimens, respectively. It is to be noted that crack width was characterized on the surface of the specimen.

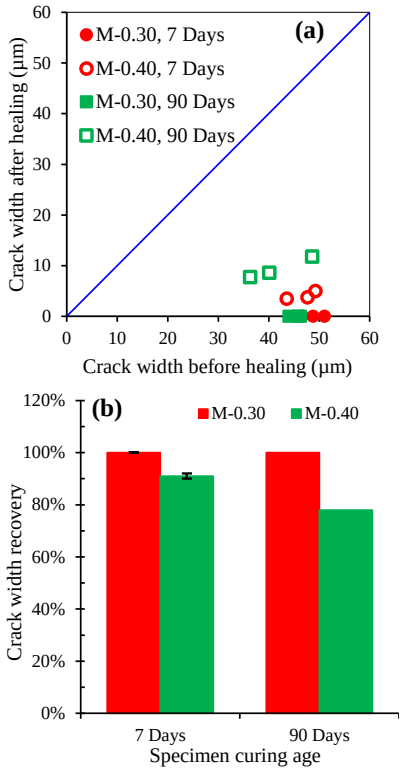

Figure 2: **(a)** Crack width healing with age in two mixtures, and **(b)** Efficiency of crack width recovery.

The crack width recovery of greater than 90% can be achieved at the early age of 7 days only. The efficiency of crack width recovery remains the same in M-0.30, whereas it decreased in matured (90 days) specimens. The crack width recovery was still greater than 80% in M-0.40 in 90 days cured specimens. Overall, a significant amount of crack sealing can be achieved in RMC-based composites at both early age and later stages of construction.

The effect of specimen age was not significant in RMC-based composites as self-healing is mainly based on carbonation reaction, and its extent does not change significantly after 7 days. The effect of the w/b ratio was more evident on the surface crack width sealing at both maturity ages, the difference being more notable in 90-day matured specimens (22%) than in 7-day matured specimens (9%). The difference is attributed to the higher content of unreacted MgO in the M-0.30 than in M-0.40, as discussed in the later section.

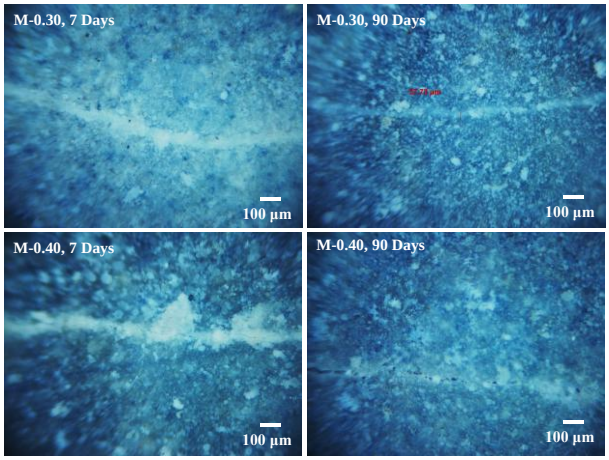

Figure 3: Surface crack sealing observed using an optical microscope.

3.2 Chemical characterization

The XRD patterns of ground samples taken from the bulk matrix of pristine specimens after ten wet/dry cycles and healed products (taken from one mm thin slice along the crack region) after ten wet/dry cycles are presented in Figure 4.

The quantitative XRD analysis of brucite (from the hydration of MgO) and periclase (unreacted MgO) in the bulk matrix and healed

products after ten wet-dry cycles is presented in Figure 5. The brucite content was higher in M-0.40 in the bulk matrix and healed products, indicating an increase in the degree of hydration with the increase in the w/b ratio. The increased brucite formation is further confirmed by the reduction in periclase content in M-0.40 compared to M-0.30. The decrease in the periclase amount in the bulk matrix also showed that further hydration reaction occurs in the bulk matrix and cracked region. The hydration reaction in the bulk matrix is facilitated through an additional supply of water during the wet-dry cycle. Thus, it can be inferred that under the self-healing regime, the recovery in the physical and mechanical performance is not solely due to the crack closure, and change in the bulk matrix phase composition also contributes partially (depending on the initial phase composition).

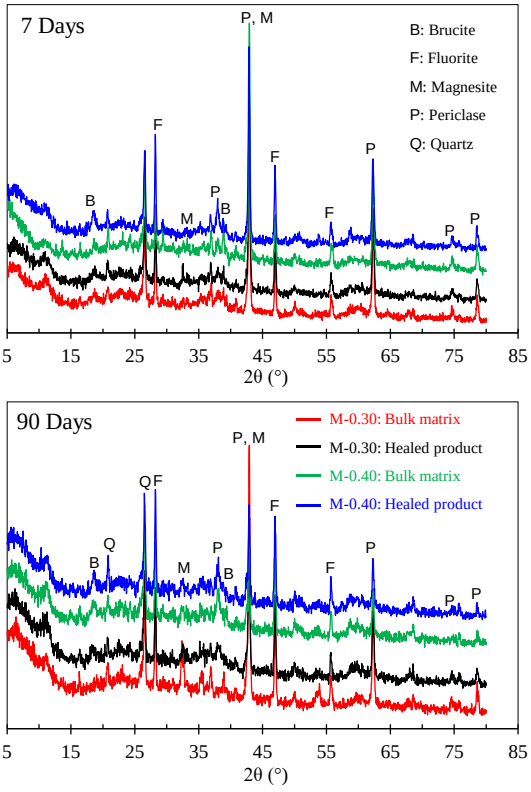

Figure 4: XRD diffractograms of the bulk matrix (after ten wet/dry cycles) and healing products.

The brucite content remained similar in M-0.30 in 7 days and 90 days matured specimens, whereas it decreased slightly in M-0.40 with age. It can be observed that the brucite content (and HMCs, as discussed later) in the bulk matrix and healed products were similar for both the composites, respectively. The similar phase composition in the bulk matrix and healed products (cracked region) suggests better compatibility between the original phase composition and newly formed products.

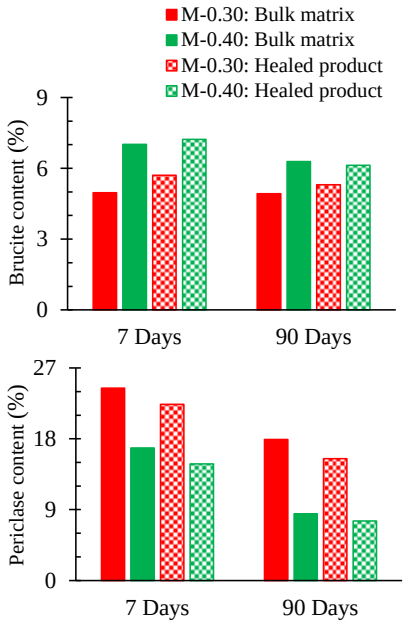

Figure 5: Brucite and Periclase content using quantitative XRD characterization.

The TGA-DTG plots of the sample collected from the bulk matrix and healed products (from initially cracked region) are shown in Figure 6. The quantitative TGA-DTG analysis (dehydroxylation and decarbonation content) is presented in Figure 7.

In RMC-based composites, dehydroxylation results from the brucite, HMCs, and M-S-H (present in minor amount) phases, and decarbonation from the HMCs phases in the range of 300-550°C. The dehydroxylation and decarbonation weight in the healed product was similar or slightly higher than that in the bulk matrix, suggesting that the exposure of the crack surface in the water contributed to the hydration of the matrix and further carbonation. The weight loss attributed to dehydroxylation and decarbonation was greater in M-0.40 than in M-0.30, aligning well with the XRD

observations. The higher brucite content in M-0.40 led to a larger amount of HMCs than in M-0.30. The increase in hydration and carbonated phases results from the unreacted MgO in the initial bulk matrix, which is consumed later during the self-healing regime, as apparent from the reduced periclase content shown in Figure 5.

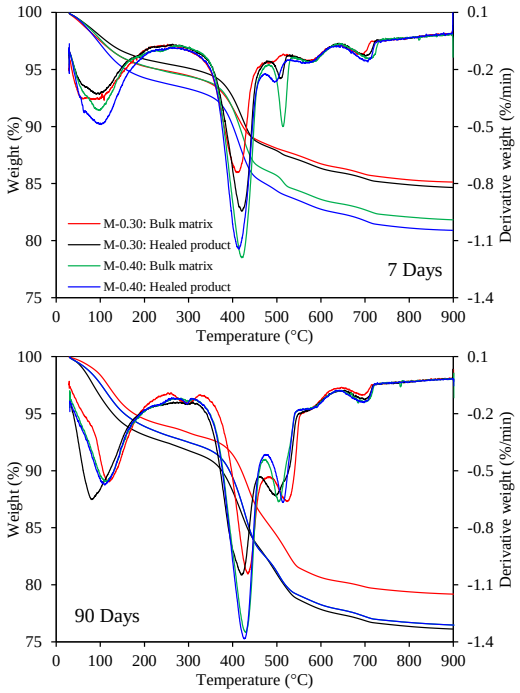

Figure 6: TGA and DTG plots of the bulk matrix (after ten wet/dry cycles) and healed products.

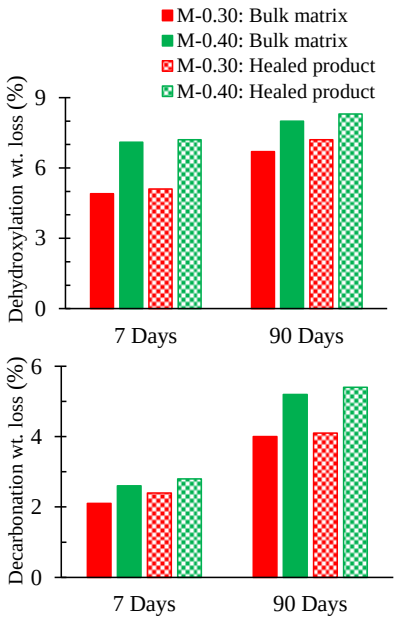

Figure 7: Dehydroxylation and decarbonation weight loss using TGA.

3.3 Morphology characterization

The SEM micrographs for studying the morphology of the healed products formed in the surface and core regions of the cracked section are presented in Figure 8 and Figure 9 for M-0.30 and M0.40, respectively.

It can be observed that the crack was densely sealed at the surface in 7-day cured M-0.30. The healing products primarily consisted of amorphous or poorly crystalline magnesium carbonate phases. The crack was also densely sealed in the core region; however, the chemical composition of the phases present was different. In the core region, the healing products include amorphous or poorly crystalline brucite and M-S-H. The morphology of healing products in the core region of 7-day cured M-0.30 was similar to M-S-H [22]. The RMC composites are generally rich in HMCs, and M-S-H phases are not formed. However, reactive silica in fly ash and moisture during the wet/dry cycle (with natural carbonation that occurs at a slower rate) could have led to M-S-H formation.

The 90-day cured M-0.30 also demonstrated good crack-sealing, with slightly different morphology of the healing products in the surface region, where amorphous phases, potentially M-S-H, were also identified (which were absent on the surface in 7-day cured specimens). The EDS analysis showed a similar chemical composition for the healing product in the surface and core region in the 90-day cured M-0.30 specimen.

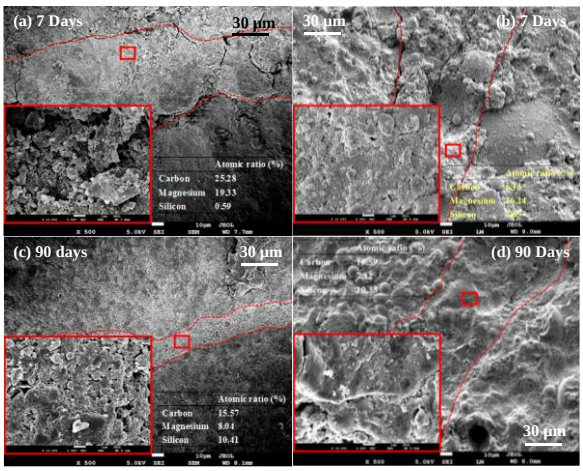

Figure 8: SEM of surface (**a** and **c**) and core (**b** and **d**) regions of healed section in M-0.30.

The crack was almost sealed at the surface and in the core region of the M-0.40 composite. The morphology of the healed products at the surface was close to hydromagnesite and dypingite. In comparison, the morphology of the healed products in the core region resembled nesquehonite, along with traces of amorphous M-S-H.

The cracks were not fully sealed in the surface and core regions in 90 days matured M-0.40 specimens compared to complete crack sealing in M-0.30. The morphology of healed products revealed the presence of mainly hydromagnesite and dypingite. The amount of amorphous M-S-H was negligible in M-0.40 compared to the significant amount observed in M-0.30. It is expected that due to the higher w/b ratio, the porosity and dissolution of MgO increased, which promoted carbonation over the formation of M-S-H phases. The surface region of M-0.40 specimens in both 7 and 90-day matured specimens was rich in carbonate phases.

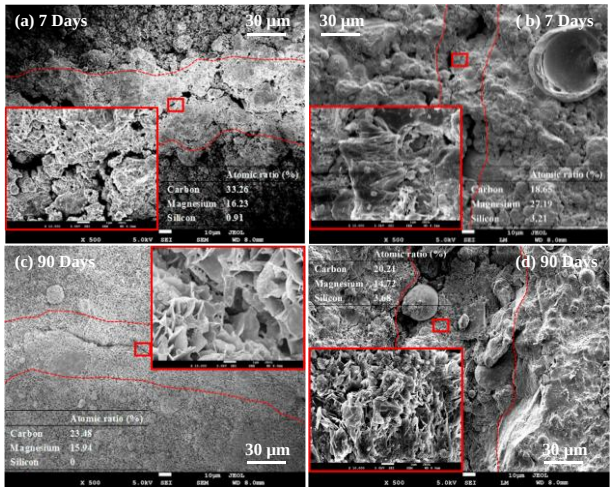

Figure 9: SEM of surface (**a** and **c**) and core (**b** and **d**) regions of healed section in M-0.40.

4 CONCLUSIONS

The study investigated the effects of water-to-binder (w/b) weight ratio on the self-healing capabilities of reactive magnesia cement (RMC) based Engineered Cementitious Composites (ECC). The key conclusions of the study based on the experimental investigation are summarized below.

- A low w/b ratio leads to better crack width recovery due to a higher amount of unreacted MgO in the cementitious matrix, which assists in self-healing on further hydration and carbonation reaction. Complete crack width recovery was observed in M-0.30 in 7- and 90-day matured specimens. The effect of specimen age on self-healing capacity was not significant in the RMC-based composite.
- The major healing products formed in RMC-based composites were hydrated magnesium carbonates (HMCs, i.e., hydromagnesite, nesquehonite, and dypingite). A minor amount of magnesium-silicate-hydrate (M-S-H) was also observed, which is not present in the initial phase composition of the carbonated RMC system.
- The morphology of healing products formed on the surface and core region differ. The healing process initiates at the surface, which restricts the supply of water and CO_2 into the core region.

A detailed comparison of the autogenous self-healing performance of OPC-based ECC (rich in calcium ions and relies on hydration for strength gain) with carbonated RMC-based ECC (rich in magnesium ions and relies on carbonation for strength gain) is presented by the authors in [21].

ACKNOWLEDGMENTS

This research was supported by the National Research Foundation (NRF) of the Republic of Singapore through a grant to the Berkeley Education Alliance for Research in Singapore (BEARS) for the Singapore-Berkeley Building Efficiency and Sustainability in the Tropics (SinBerBEST) program.

REFERENCES

[1] Liska, M., Vandeperre, L., Al-Tabbaa, A., 2008. Influence of carbonation on the properties of reactive magnesia cement-based pressed masonry units. *Adv. Cem. Res.* 20(2), 53-64.

[2] Liska, M., Al-Tabbaa, A., 2009. *Ultra-green construction: reactive magnesia masonry products*, Proceedings of the Institution of Civil Engineers-Waste and Resource Management. Thomas Telford Ltd, pp. 185-196.

[3] Vandeperre, L., Al-Tabbaa, A., 2007. Accelerated carbonation of reactive MgO cements. *Adv. Cem. Res.* 19(2), 67-79.

[4] Unluer, C., Al-Tabbaa, A., 2013. Impact of hydrated magnesium carbonate additives on the carbonation of reactive MgO cements. *Cem. Concr. Res.* 54, 87-97.

[5] Unluer, C., Al-Tabbaa, A., 2014. Enhancing the carbonation of MgO cement porous blocks through improved curing conditions. *Cem. Concr. Res.* 59, 55-65.

[6] Ruan, S., Qiu, J., Yang, E.-H., Unluer, C., 2018. Fiber-reinforced reactive magnesia-based tensile strain-hardening composites. *Cem. Concr. Compos.* 89, 52-61.

[7] Li, V.C., 1997. *Engineered cementitious composites (ECC)-tailored composites through micromechanical modeling*, in: N. Banthia, A. Bentur, a.A.M. (Eds.), Fiber Reinforced Concrete: Present and the Future. Canadian Society of Civil Engineers.

[8] Li, V.C., 2003. On engineered cementitious composites (ECC) a review of the material and its applications. *J. Adv. Concr. Tech.* 1(3), 215-230.

[9] Li, V.C., 2008. *Engineered cementitious composites (ECC) material, structural, and durability performance,* in: Nawy, E.G. (Ed.) Concrete Construction Engineering Handbook. CRC Press, pp. 1023-1070.

[10] Kan, L.-L., Shi, H.-S., Sakulich, A.R., Li, V.C., 2010. Self-Healing Characterization of Engineered Cementitious Composite Materials. *ACI Mater. J.* 107(6).

[11] Sahmaran, M., Yildirim, G., Erdem, T.K., 2013. Self-healing capability of cementitious composites incorporating different supplementary cementitious materials. *Cem. Concr. Compos.* 35(1), 89-101.

[12] Yang, Y., Lepech, M.D., Yang, E.-H., Li, V.C., 2009. Autogenous healing of engineered cementitious composites under wet–dry cycles. *Cem. Concr. Res.* 39(5), 382-390.

[13] Qian, S., Zhou, J., Schlangen, E., 2010. Influence of curing condition and precracking time on the self-healing behavior of Engineered Cementitious Composites. *Cem. Concr. Compos.* 32(9), 686-693.

[14] Özbay, E., Sahmaran, M., Yücel, H.E., Erdem, T.K., Lachemi, M., Li, V.C., 2013. Effect of sustained flexural loading on self-healing of engineered cementitious composites. *J. Adv. Concr. Tech.* 11(5), 167-179.

[15] Yang, Y., Yang, E.-H., Li, V.C., 2011. Autogenous healing of engineered cementitious composites at early age. *Cem. Concr. Res.* 41(2), 176-183.

[16] Van Tittelboom, K., Gruyaert, E., Rahier, H., De Belie, N., 2012. Influence of mix composition on the extent of autogenous crack healing by continued hydration or calcium carbonate formation. *Constr. Build. Mater.* 37, 349-359.

[17] Qiu, J., Tan, H.S., Yang, E.-H., 2016. Coupled effects of crack width, slag content, and conditioning alkalinity on autogenous healing of engineered cementitious composites. *Cem. Concr. Compos.* 73, 203-212.

[18] Wu, H.-L., Zhang, D., Ellis, B.R., Li, V.C., 2018. Development of reactive MgO-based Engineered Cementitious Composite (ECC) through accelerated carbonation curing. *Constr. Build. Mater.* 191, 23-31.

[19] Qiu, J., Ruan, S., Unluer, C., Yang, E.-H., 2019. Autogenous healing of fiber-reinforced reactive magnesia-based tensile strain-

hardening composites. *Cem. Concr. Res.* 115, 401-413.

[20] Li, V.C., Wu, C., Wang, S., Ogawa, A., Saito, T., 2002. Interface tailoring for strain-hardening polyvinyl alcohol-engineered cementitious composite (PVA-ECC). *Mater. J.* 99(5), 463-472.

[21] Gu, L., Kumar, D., Unluer, C., Monteiro, P.J.M., Yang, E.-H., 2024. Autogenous healing efficiency of calcium (OPC) and magnesium (MgO) binder-based strain-hardening cementitious composite (SHCC). *Cem. Concr. Compos.* (Under Review).

[22] Sonat, C., Unluer, C., 2019. Development of magnesium-silicate-hydrate (MSH) cement with rice husk ash. *J. Clean. Prod.* 211, 787-803.